

Controllable light-induced conic structures in silicon nanowire arrays by metal-assisted chemical etching

This content has been downloaded from IOPscience. Please scroll down to see the full text.

2014 Nanotechnology 25 025602

(<http://iopscience.iop.org/0957-4484/25/2/025602>)

View [the table of contents for this issue](#), or go to the [journal homepage](#) for more

Download details:

IP Address: 202.120.52.96

This content was downloaded on 16/12/2013 at 04:30

Please note that [terms and conditions apply](#).

Controllable light-induced conic structures in silicon nanowire arrays by metal-assisted chemical etching

Shenli Zhang, Xinwei Wang, Hong Liu and Wenzhong Shen

Laboratory of Condensed Matter Spectroscopy and Opto-Electronic Physics, and Key Laboratory of Artificial Structures and Quantum Control (Ministry of Education), Department of Physics and Astronomy, and Institute of Solar Energy, Shanghai Jiao Tong University, 800 Dong Chuan Road, Shanghai 200240, People's Republic of China

E-mail: liuhong@sjtu.edu.cn and wzshen@sjtu.edu.cn


Received 18 July 2013, in final form 4 November 2013

Published 12 December 2013

Abstract

Silicon nanowires (SiNWs) have long been considered a promising material due to their extraordinary electrical and optical properties. As a simple, highly efficient fabrication method for SiNWs, metal-assisted chemical etching (MACE) has been intensively studied over recent years. However, effective control by modulation of simple parameters is still a challenging topic and some key questions still remain in the mechanistic processes. In this work, a novel method to manipulate SiNWs with a light-modulated MACE process has been systematically investigated. Conic structures consisting of inclined and clustered SiNWs can be generated and effectively modified by the incident light while new patterns such as 'bamboo shoot' arrays can also be formed under certain conditions. More importantly, detailed study has revealed a new top-down 'diverting etching' model of the conic structures in this process, different from the previously proposed 'bending' model. As a consequence of this mechanism, preferential lateral mass transport of silver particles occurs. Evidence suggests a relationship of this phenomenon to the inhomogeneous distribution of the light-induced electron-hole pairs beneath the etching front. Study on the morphological change and related mechanism will hopefully open new routes to understand and modulate the formation of SiNWs and other nanostructures.

Keywords: light-modulated, inclined and clustered silicon nanowires, metal-assisted chemical etching, formation process

 Online supplementary data available from stacks.iop.org/Nano/25/025602/mmedia

(Some figures may appear in colour only in the online journal)

1. Introduction

Nanostructures in silicon material have attracted intensive research due to their academic and industrial importance. Silicon nanowires (SiNWs), due to their natural semiconducting properties along with special nanoscale opto-electronic effects, have become a promising material for application in many areas, such as photovoltaics [1, 2], electronics [3, 4], biology [5] and photocatalysis [6]. Various physical and chemical methods have been investigated to fabricate SiNWs

during the recent decades, including vapor-liquid-solid (VLS) growth, the supercritical fluid-phase approach, reactive ion etching (RIE), metal-assisted chemical etching (MACE), etc [7–11]. Amongst these, MACE has become one of the most economical and convenient methods due to its feasibility with low equipment requirement and adaptability for industrial fabrication [12–14]. Compared with other routes, for instance the commonly used VLS growth, the MACE method has a higher production rate but poorer controllability. Understanding and modulation of the formation process

in this method have remained challenging topics for the desired architecture modification, which is important for the fabrication of new devices based on the SiNWs.

To date, ordered SiNWs by the MACE method are normally realized with the involvement of templates [15–18], and various slant directions have been obtained by taking advantage of crystalline orientation [19, 20] or by modifying the metal catalysts used [21]. Besides, the reactant ratios, surface tension force and temperature have also been tuned in order to further adjust the nanowire dimensions or to create new structures such as inclined wires [22–24], hooked and ground-collapsed shapes [25], curved forms with controlled turning angles [26] and nanopillars with nanoporous shells [27]. The control of MACE is normally investigated with variation of the chemical factors of the system, which is simple and direct, but its efficiency is often limited by the interactions between different coexisting factors (etching rate, etching direction, etc) in the reaction–diffusion process [13, 28, 29]. Moreover, in previous research on morphology control and mechanism, ordered nanostructure modification has often relied on existing structures with similar symmetries (patterned microstructure, anisotropic properties of crystal orientation, etc). Therefore, in general, the routes to control this method have often been complex, expensive and required strong support from templates. Besides, many questions also remain concerning the complicated mechanisms in the morphological and structural change in efforts to control MACE [8, 26, 27, 30]. Notably, the involvement of photons can be quite an effective way to influence the MACE process, since Si is a semiconducting material with a narrow bandgap, and has exhibited a noticeable function in the photocatalysis, as also revealed by Osgood *et al* [31] regarding the photon effect on accelerating the etching rate of compound semiconductors, with the same effect recently reported on both N- and P-type silicon by Huang *et al* [8]. Nevertheless, its character in the morphological evolution is still seldom known, although it can be a very important key to morphology control and mechanistic research.

Herein, we report a controllable light-modulated MACE method to fabricate inclined and clustered SiNWs for the first time. Systematic investigations have revealed that the inclination angle, growth rate and cluster shape of the SiNWs can be significantly influenced by the light parameters and doping level. New structures such as a ‘bamboo shoot’ like pattern could also be established with simple adjustment of parameters. More importantly, we have found through detailed *in situ* investigation that the formation of inclination and clustering in this process is likely not through the normally considered ‘bending’ model [25], but rather due to a preferential lateral movement of reaction fronts (accompanied by subsequent motion of silver particles) at the bottom of the Si wires (here ‘lateral’ refers to the direction parallel to the surface of the substrate while conventional ‘vertical’ etching is perpendicular to the surface). Evidently, significant mass transport of the Ag results and can be detected by energy-dispersive x-ray spectroscopy (EDX) measurement on the surface of the Si substrate. We have proposed a possible explanation for the origin of this phenomenon, namely that

it might have been induced by the anisotropic distribution of the light-induced electron–hole pairs at the Si surface due to an inhomogeneous initial light distribution, which was later influenced by the morphological evolution of the SiNWs. This can also well explain the effect of the light parameters and doping level on the modification of the SiNW arrays. Based on this model, more structural manipulation can be expected if further modification of the light is applied, and a similar mechanism exists in other nanostructure formation in SiNWs or other materials.

2. Experimental section

In this work, the silicon samples were intrinsic ($\rho > 5000 \Omega \text{ cm}$) and phosphorous doped N-type (with resistivities of 1–10, 0.1 and $0.01 \Omega \text{ cm}$) with crystal orientation of (001) and size of $1 \text{ cm} \times 1 \text{ cm}$. These substrates were washed by sonication in acetone and ethanol for 30 min each. Then they were immersed in an aqueous solution of 0.04 M silver nitrate (AgNO_3) and 3.7 M hydrofluoric acid (HF) for 20 s to deposit silver nanoparticles (AgNPs) onto the surface at room temperature ($T = 20^\circ\text{C}$). Subsequently, the silicon pieces were washed with deionized water (DI water) and immediately immersed in the etching solution composed of 4.6 M HF and 0.6 M hydrogen peroxide (H_2O_2) for 15 min.

The illumination was introduced during the etching process, mostly provided by the applied light source from a semiconductor laser device with power ranging from 10 to 85 mW and wavelengths of 405, 532, 650 and 980 nm. The laser beam passed through a series of beam expanding lenses and was expanded to 0.5 cm in diameter (spot size about 0.785 cm^2). Other applied illumination devices were light bulbs and an AM 1.5 light source from a solar simulator (Oriel Sol 2 A). When the etching was over, the samples were dipped into diluted nitric acid (HNO_3 , 1:1 v/v) to remove residual Ag nanoparticles and then rinsed with DI water. The morphology of the as-fabricated SiNWs was characterized by a scanning electron microscope (SEM, FEI SIRION 200). The chemical analysis was carried out by EDX in the same machine under 15 kV. The illumination power of the laser was measured by a 200–1100 nm Thorlabs optical power meter.

3. Results and discussion

3.1. Patterns with/without illumination

Prior to the introduction of light, vertically aligned SiNWs were grown using the MACE method. As shown in figure 1(a), the nanowires have characteristic lengths of about $4.8 \mu\text{m}$ and widths of about 60–100 nm. After the introduction of light into the MACE system, significant morphological change resulted, in the form of spatial inhomogeneity (such as clustering and etching) and morphological deformation (inclination and curvature) in the nanowire arrays (figures 1(b)–(f)).

Specifically, the inclination and clustering of SiNWs is an iconic phenomenon with the injection of light. It could take place when a heavily doped Si wafer was illuminated

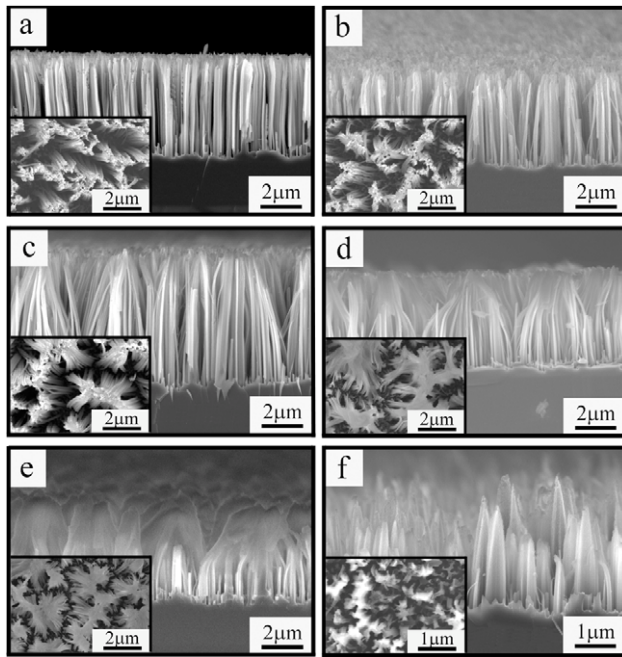


Figure 1. SEM images (side view) of various morphologies obtained under different illumination conditions. The insets are top views. (a) Intrinsic SiNWs fabricated under dark conditions. (b) SiNWs (substrate resistivity $0.01 \Omega \text{ cm}$) fabricated under illumination with a 20 W bulb. (c) SiNWs (substrate resistivity $0.01 \Omega \text{ cm}$) fabricated under illumination with a 250 W bulb. (d) SiNWs (substrate resistivity $0.01 \Omega \text{ cm}$) fabricated under illumination with a 10 mW illumination power laser. The wavelength is 650 nm. (e) SiNWs (substrate resistivity $0.01 \Omega \text{ cm}$) fabricated under illumination with a 45 mW illumination power laser. The wavelength is 650 nm. (f) Intrinsic SiNWs fabricated under AM 1.5 illumination.

by a 20 W bulb (figure 1(b)). Moreover, this phenomenon could also appear with a certain curvature of the SiNWs if a higher power (250 W) bulb was applied, and the density of the clustering became lower (figure 1(c)). This phenomenon became more apparent when the light source was changed to a 10 mW laser with a wavelength of 650 nm (figure 1(d)). The density of the clustering became even lower if a stronger laser (45 mW, 650 nm) was applied. Meanwhile, some 'melt-down' like phenomena emerged on top of the clustered SiNWs, as shown in figure 1(e). However, under some special cases (e.g., AM 1.5 illumination), the clustering can disappear and a particular 'bamboo shoot' pattern can form, in which thick (200–300 nm) columns with varying lengths develop instead of thin (60–100 nm) SiNWs (figure 1(f)). For a certain chemical condition, these different formations were in general determined by the wavelength and power density of the incident light, as well as the doping condition of the Si substrate. We will demonstrate the systematic tunable nature of these factors in the following sections.

3.2. Effect of illumination power

3.2.1. Substrate resistivity: 1–10 $\Omega \text{ cm}$, wavelength: 650 nm.

The first investigation was on the behavior of SiNW formation under varying illumination power. For identical initial

conditions, the experiment was performed on a lightly doped (1–10 $\Omega \text{ cm}$) N-Si substrate and the laser wavelength was fixed at 650 nm (red), which is a common component in the natural light spectrum. Generally, significant morphological change took place in the as-grown SiNWs under illumination compared to those without illumination, as demonstrated by the SEM images in figure 2. The SiNWs have changed from an almost vertical ordered array (figures 2(a) and (b)) to inclined and clustered nanowire bunches (figures 2(c)–(h)). On one hand, the deflection angle (whose definition can be seen in the supporting information, figure S2 available at stacks.iop.org/Nano/25/025602/mmedia) on top of the clustered nanowires became gradually larger, as shown in figures 2(a)–(f). On the other hand, the clustering density (its definition can also be found in the supporting information, figure S3 available at stacks.iop.org/Nano/25/025602/mmedia) became lower with increasing illumination power.

Furthermore, to describe this morphological behavior in a more quantitative way, we have measured two values at each illumination power point (0, 10, 20, 35, 45, 70 and 85 mW). As shown in figures 2(i) and (j), the deflection angle increased drastically when the illumination power increased from 0 to 10 mW and then this increase slowed down for illumination power higher than 10 mW. Finally, when the power reached 85 mW, the deflection angle tended to reach a certain saturation value. In contrast, the clustering density showed an initially drastic decrease versus increasing illumination power (less than 45 mW) and then this decrease gradually slowed down. Moreover, the tendency to form a 'melt-down' type surface on top of the clustering can also be observed as the incident power is increased, although not as strong as the case shown in figure 1(e). Finally, the growth rate of the SiNWs increases with increasing illumination power. As shown in figure 2(i), the length of the SiNWs increased from 4.04 to 5.84 μm when the power of the light increased from 10 to 85 mW.

3.3. Effect of photon energy

3.3.1. Substrate resistivity: 1–10 $\Omega \text{ cm}$, illumination power: 20 mW.

The previous experiment has shown a significant influence of the light power (or photon number) on the morphology of the SiNWs. This is then followed by the question whether the photon energy has a significant influence on the SiNW formation as well. For identical conditions, lasers with various wavelengths were applied to illuminate the reacting Si substrate with a fixed spot area (0.785 cm^2) and a typical power of 20 mW. Four wavelengths were chosen: 980 nm (infrared), 650 nm (red), 532 nm (green) and 405 nm (violet). As shown in figure 3, varying the light wavelength (or photon energy) also has a significant influence on the SiNW formation. When the incident light was infrared (980 nm, figures 3(a) and (b)), the as-formed SiNWs were only slightly inclined and the clustering shape was not significant, similarly to the situation without any illumination. When the photon energy was higher (650 nm), the inclination of the SiNWs and the clustering became stronger, together with a certain curvature of the SiNWs (figures 3(c) and (d)). This trend

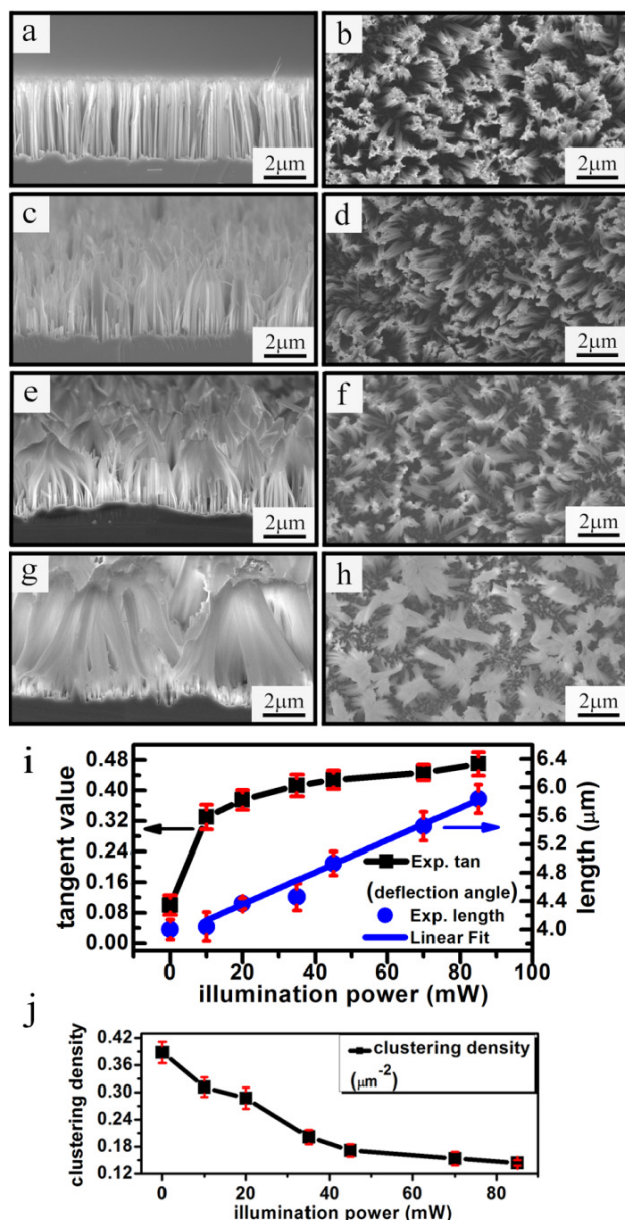


Figure 2. Influence of illumination power on the formation of SiNWs. (a)–(h) SEM images (side view and top view) of SiNWs obtained under different illumination powers. (a), (b) No illumination. (c), (d) 10 mW illumination power. (e), (f) 35 mW illumination power. (g), (h) 85 mW illumination power. (i) Tangent value of the deflection angle and length of SiNWs versus illumination power. (j) Clustering density versus illumination power.

became even greater when green light (532 nm) was incident, as shown in figures 3(e) and (f). In the meantime, the clustering density decreased from 0.44 to 0.19 μm^{-2} when the light wavelength changed from 980 to 532 nm.

Nevertheless, drastic change took place when the surface was illuminated by violet light (405 nm). Under this condition the SiNWs appeared as short and sharp columns with reasonably different lengths, similar to the ‘bamboo shoot’ pattern obtained under AM 1.5 illumination but with smaller column size. Finally, we have to consider the fact that in this experiment an increase of the photon energy was

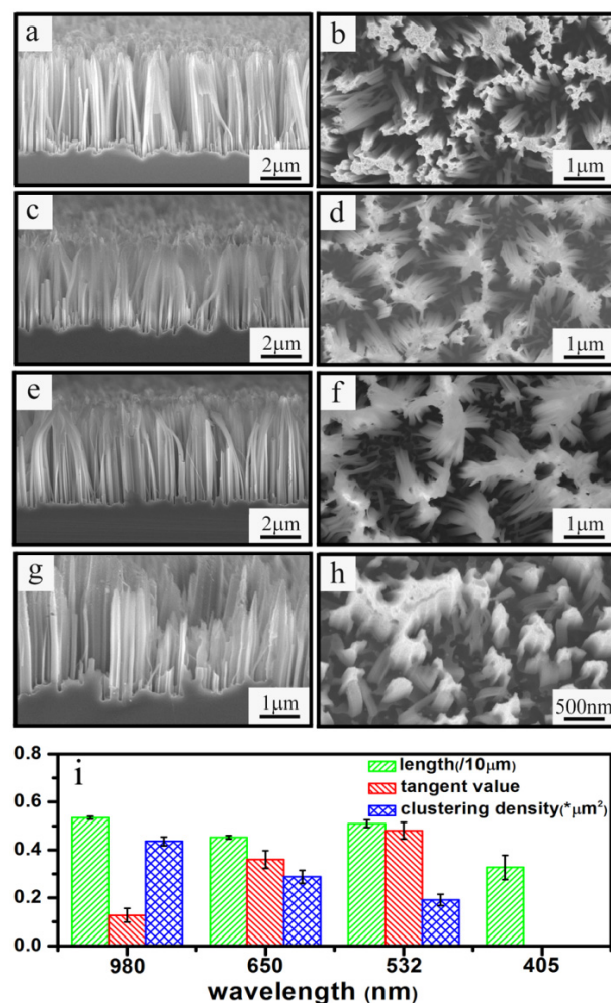


Figure 3. Influence of photon energy on the formation of SiNWs. (a)–(h) SEM images (side view and top view) of SiNWs obtained under different wavelengths. (a), (b) 980 nm. (c), (d) 650 nm. (e), (f) 532 nm. (g), (h) 405 nm. (i) Length, tangent value of the deflection angle and clustering density of SiNWs under illumination with different wavelengths, where non-dimensional relative units are used for these values for easy comparison.

accompanied by a decrease of the photon number when we kept the total light power fixed. If we consider the similar morphological change with increasing photon number in the previous experiment, we can draw a first conclusion that increase of the photon energy has at least as strong an effect as that of the photon number on the SiNWs. With increasing photon energy, inclination and clustering appeared and became stronger. However, as also shown in figure 3(i), the length of the SiNWs decreased with increasing photon energy, which is contradictory to the result with increasing photon number. This contradiction might be due to reduced photon number or enhanced etching on the top position of the SiNWs with high-energy photons.

3.4. Influence of doping level

3.4.1. Wavelength: 650 nm, illumination power: 20 mW.

Apparently, the wavelength and power of the incident light

can both significantly influence the formation of SiNWs. Moreover, the results presented in figure 1 have also shown variation of the SiNWs under different doping levels of the Si substrate, which indicates the involvement of the electronic properties of the silicon material. Therefore, it is also necessary to study the influence of the doping level and this can hopefully further aid in our understanding of the mechanism of the structure formation under illumination. According to the previous investigations, light with $\lambda = 650$ nm and a power of 20 mW was chosen as the constant condition. As shown in figure 4, inclination and clustering of the SiNWs took place for all doping levels of the Si substrate with illumination, while detailed differences still existed among the cases. When the substrate was intrinsic, the Si wires were quite distinguishable and ordered. As the doping level increased, the top of the clustering became smoother, and the nanowires became ambiguous, until an almost ‘melt-down’ like pattern appeared for the heaviest doping (0.01 Ω cm). Meanwhile, the reaction fronts at the bottom of the SiNWs became more and more irregular. For the heaviest doping at 0.01 Ω cm, the reaction fronts had an appearance similar to the ‘viscous fingering’ shape [32] and went deeper through the substrate than the average depth of the nanowire bottoms, which implies strong dissolving at the reaction fronts. Furthermore, as the doping level increased from intrinsic to 0.01 Ω cm, the clustering density in general decreased from 0.34 to 0.14 μm^{-2} , similarly to the trend as the wavelength of the incident light decreased. Finally, the growth rate of the SiNWs was not significantly changed for different doping levels.

In terms of all the above results, it is clear that change of the incident light can induce significant modification on the formation of the SiNW arrays. Therefore, variation of the light parameters apparently offers an effective means for the control of MACE. Several key points can be herein addressed. First, for a fixed light wavelength, the inclination and clustering were both enhanced with increasing illumination power, i.e., increasing photon number. Meanwhile, a similar tendency also appeared with increasing photon energy. Considering that the photon number decreased with photon energy at fixed power, the influence of higher photon energy on the morphology of SiNWs for fixed photon number will be even greater. Second, the net growth rate of SiNWs significantly increased with increasing illumination power, while it showed contradictory tendencies for SiNWs etched under varying wavelength at fixed illumination power. This implies that the photon number and energy might have influenced different steps in the process. Noticeably, the inclination of SiNWs by illumination was normally accompanied by a certain curvature. Moreover, the ‘melt-down’ phenomenon (which means a smoothed top surface of the clustering) occurred if the illumination power was quite intense. Finally, excessive illumination can deteriorate the inclination and clustering of SiNWs and form a ‘bamboo shoot’ like pattern. To understand the insight from these phenomena, more investigations would be necessary prior to the modeling of this process.

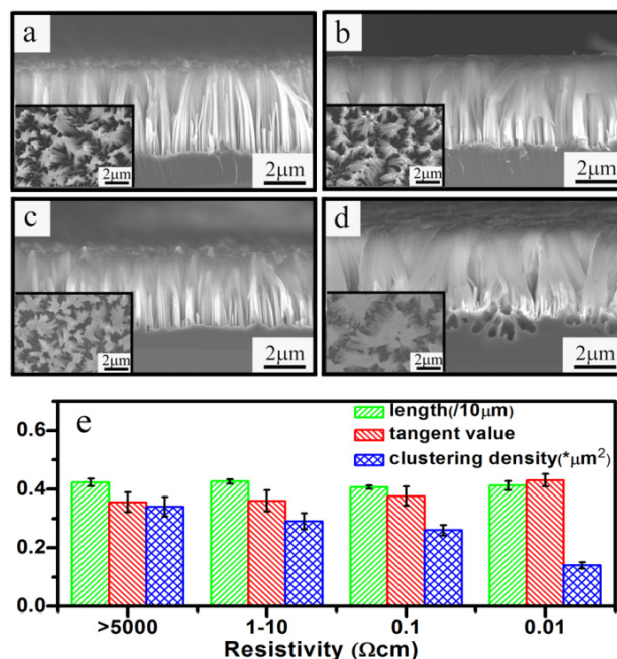


Figure 4. SEM images (side view) of SiNWs obtained with different doping levels. (a) Intrinsic substrate. (b) N-type substrate with resistivity of 1–10 Ω cm. (c) N-type substrate with resistivity of 0.1 Ω cm. (d) N-type substrate with resistivity of 0.01 Ω cm. (e) Length, tangent value of the deflection angle and clustering density of SiNWs for four doping levels, where for the length and clustering density, non-dimensional relative units are used for easy comparison.

3.5. Influence of other factors and study of the microporosity change

In experiments with the involvement of a laser, a significant parameter is the effect of the light-induced heat, which might influence the chemical reactions during the etching process [33]. Two experiments were carried out with respect to this: (1) the local heat effect induced by the laser spot; (2) the influence of temperature rise on the reaction in this experiment. For the first experiment, a K-type thermocouple was made in contact with the Si surface beside the illuminated area, and no significant temperature rise was detected within the experimental precision (1 $^{\circ}\text{C}$) under different illumination powers and different wavelengths (described in sections 3.2 and 3.3). Secondly, a SiNW fabrication process without illumination was carried out under a series of different temperatures (19, 25, 35, 45 $^{\circ}\text{C}$). However, no significant size and morphology change emerged with these various temperatures (details can be found in the supporting information, figure S5 available at stacks.iop.org/Nano/25/025602/mmedia). Therefore, the heat effect due to the laser beam can be ruled out in this experiment.

Moreover, for various nanopillar structures, the capillary force is often an important factor which induces significant morphological changes [19, 34]. For instance, the work of Berggren's group has shown techniques to produce clustered SiNWs by capillary forces [24]. To study its involvement in the inclination and clustering phenomena here, we have

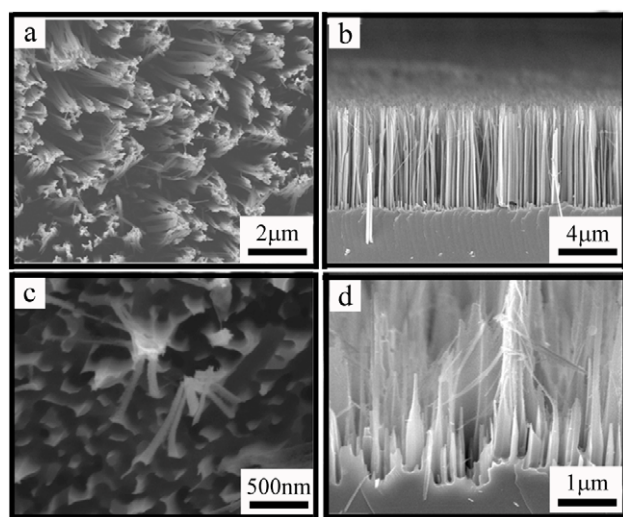


Figure 5. SEM images (top view and side view) of SiNWs (N100 1–10 Ω cm) after immersion in *aqua regia* solution (1 min) followed by HF solution. (a), (b) SiNWs fabricated without illumination. (c), (d) SiNWs fabricated under 650 nm, 20 mW laser illumination.

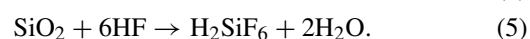
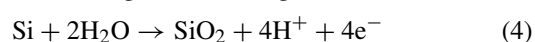
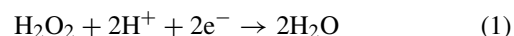
carried out supercritical CO_2 drying experiments which eliminate possible capillary force by avoiding meniscus formation. However, the inclination and clustering still survived even after the application of the supercritical CO_2 (see the supporting information, figure S6 available at stacks.iop.org/Nano/25/025602/mmedia). Therefore, it seems that the capillary force is not a dominant factor in the formation of inclination and clustering of SiNWs.

Also, as porosity is an important parameter for both understanding the reaction process and various applications, it is worthwhile to obtain preliminary results on the effect of illumination on the porosity of SiNWs. The nanoporosity of the samples was studied by an oxidation/HF attacking experiment [25]. Samples (with/without inclination and clustering) were firstly exposed to *aqua regia* ($\text{HCl}:\text{HNO}_3$ 3:1 v/v) for 1 min, and then soaked in saturated HF for 1 min. As shown in figure 5, two facts are worth noting. On one hand, strong etching has taken place on the sample with inclination and clustering by illumination, indicating much enhanced porosity compared to the sample without illumination (which can also be detected by the PL measurement in the supplementary information, figure S7 available at stacks.iop.org/Nano/25/025602/mmedia). On the other hand, the etching shown in figures 5(c) and (d) occurred irregularly at different positions on the SiNWs. Therefore, illumination during the etching process generally increases the porosity of the top part of SiNWs, while the influential depth seems to be inhomogeneous for different SiNWs.

4. Mechanism study

Apparently, the studies on the morphological change of SiNWs with illumination in section 3.5 have ruled out any dominant effect of the heat or capillary force, which suggests other factors and related mechanisms. To understand and possibly control this phenomenon, further *in situ*

investigations are then needed on the physical–chemical processes that underlie it. For a typical MACE reaction, H_2O_2 and Ag^+ cations are reduced at the cathode site (i.e. the Ag nanoparticles), and Si is oxidized at the anode site (Si/Ag interface) which would be subsequently dissolved by HF [35, 36]. Besides, there also exists another reaction route, in that H_2O_2 directly oxidizes the Si without the involvement of Ag at a much slower rate. The main reactions in the $\text{HF}-\text{H}_2\text{O}_2-\text{H}_2\text{O}$ system are as follows:



Considering this mechanism, SiNWs would result when the Si substrate is only partly covered by metal particles, which makes the etching process of Si beneath the particles much faster than that in the area without them [8].

When light with energy higher than the Si bandgap (1.12 eV) is incident, it can first excite electron–hole pairs in the silicon (adjacent to the surface). This means that the energy of the electrons in the Si becomes higher (excited from the valence band to the conduction band) and can be more easily released to the oxidizing species (Ag^+ and H_2O_2). Furthermore, the photo-generated holes enhance the dissolution of silicon at the same time [37]. This can then significantly accelerate the charge transfer from Si to Ag^+ , and thus promotes the etching rate at the bottom of the Si wires. Supposing that the top of the nanowires is not significantly influenced, the net growth of the nanowires can therefore be accelerated. It can be naturally speculated that this process becomes stronger when more photons are injected, which is also supported by figure 2(i). In the experiment with varying photon energy, the illumination power was fixed, so the photon number decreased as the photon energy increased. Although increase of the photon energy can probably generate more high-energy electrons, apparently its influence on the enhancement of nanowire growth is weaker than increase of photon number (figure 3(i)).

As indicated by the results discussed in section 3, the most significant phenomenon is the variability of the inclination and clustering of the SiNWs by incident light and the preliminary doping level of the sample. Similar inclination and clustering of SiNWs have been found in pure chemical systems under different solution ratio or different substrate type conditions [20, 22, 27], whose detailed establishment has seldom been reported. A certain SiNW bending by a different technique was studied in a recent paper [25], where it was assigned to a mechanical deformation due to a drastic porosity change at a certain height of the SiNWs. To investigate this, a time evolution experiment is then proposed for SiNWs under a certain illumination. Suppose the inclination of the SiNWs in this experiments is a ‘bending’ process [25], then a time point t_c would exist at which the SiNWs began to bend and before which the SiNWs were still straight. This time point is measurable through a series of SEM images taken at different

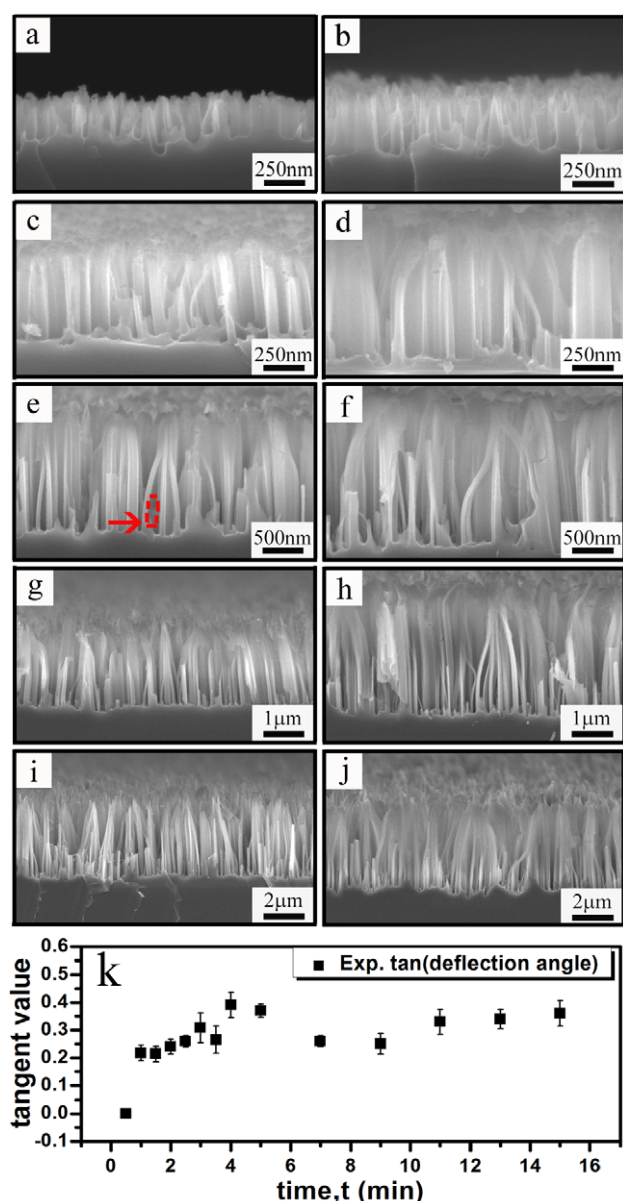


Figure 6. SEM images (side view) of SiNWs obtained at different time points: (a) 5 s, (b) 15 s, (c) 30 s, (d) 1 min, (e) 2 min, (f) 3.5 min, (g) 5 min, (h) 9 min, (i) 11 min, (j) 15 min. (k) Tangent value of deflection angle versus time.

time stages, as at a certain stage we should see the morphology of the SiNWs change from vertical to 'bent'. Secondly, if the curvature of the SiNWs is due to a 'bending' process, then the SiNWs would appear to be still straight below the bending point. Samples were fabricated under the same etching and illumination conditions (650 nm wavelength with 20 mW illumination power and resistivity of 1–10 Ω cm) at a set of etching time points between 0 and 15 min (5 s, 15 s, 30 s, 1 min, 1 min and 30 s, 2 min, 2 min and 30 s, 3 min, 3 min and 30 s, 4 min, 5 min, 7 min, 9 min, 11 min, 13 min, 15 min). The morphology and dimension properties were characterized and are shown in figures 6 and 7.

On one hand, the lateral view in figure 6 indicates that inclination and clustering of SiNWs have taken place at the

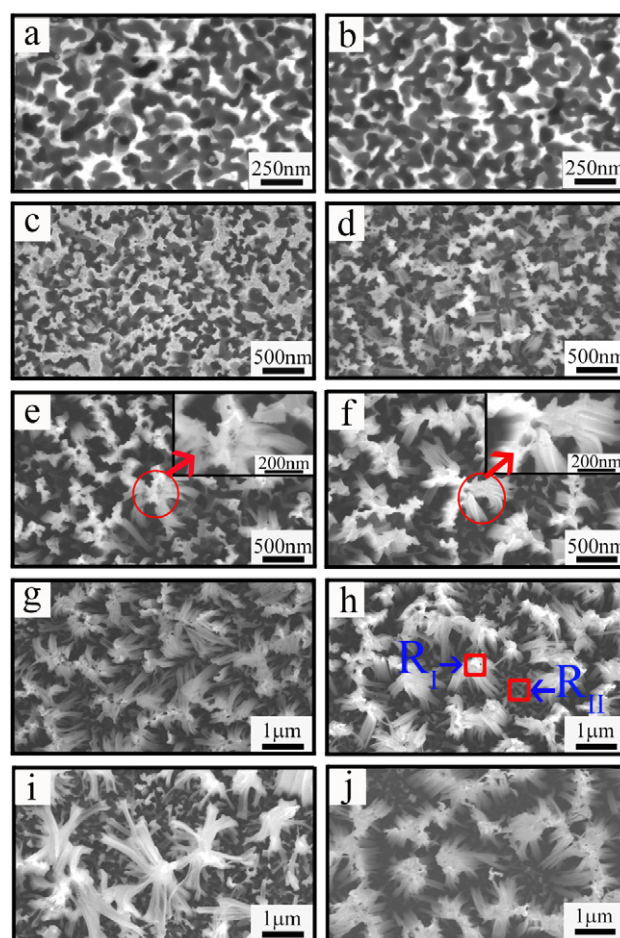


Figure 7. SEM images (top view) of SiNWs obtained at different time points: (a) 5 s, (b) 15 s, (c) 30 s, (d) 1 min, (e) 2 min (the inset is a zoomed-in image), (f) 3 min and 30 s (the inset is a zoomed-in image), (g) 5 min, (h) 9 min, (i) 11 min, (j) 15 min.

very beginning of the etching process. It can be also seen that no significant time point can be found for a sudden 'bending' event throughout the experiment and the inclination of the SiNWs gradually continued during the whole process. This strongly indicates that the 'bending' model is not likely to be applicable in this system, i.e., the inclination under illumination is actually different from a 'bending' deformation due to a structural weakness at a certain height of the nanowires in the middle of the reaction. On the other hand, as shown by the top view in figure 7, the size of the nanowire clustering became larger and more nanowires aggregated in one cluster during the growth process, while the clustering density continued to decrease (indicated by the statistical graph in figure 8(a)). Therefore, it can be concluded that a certain kind of 'expansion' process has seemingly taken place at the bottom of the nanowires if one considers these facts together with the invariability of the deflection angle versus time and variation versus the light and doping level. The slope of this expansion was not dependent on time or crystallographic anisotropy, but was dependent on the light and chemical parameters.

As evidence, in figure 6(e), some sort of spacing expansion has taken place at the marked position. In other

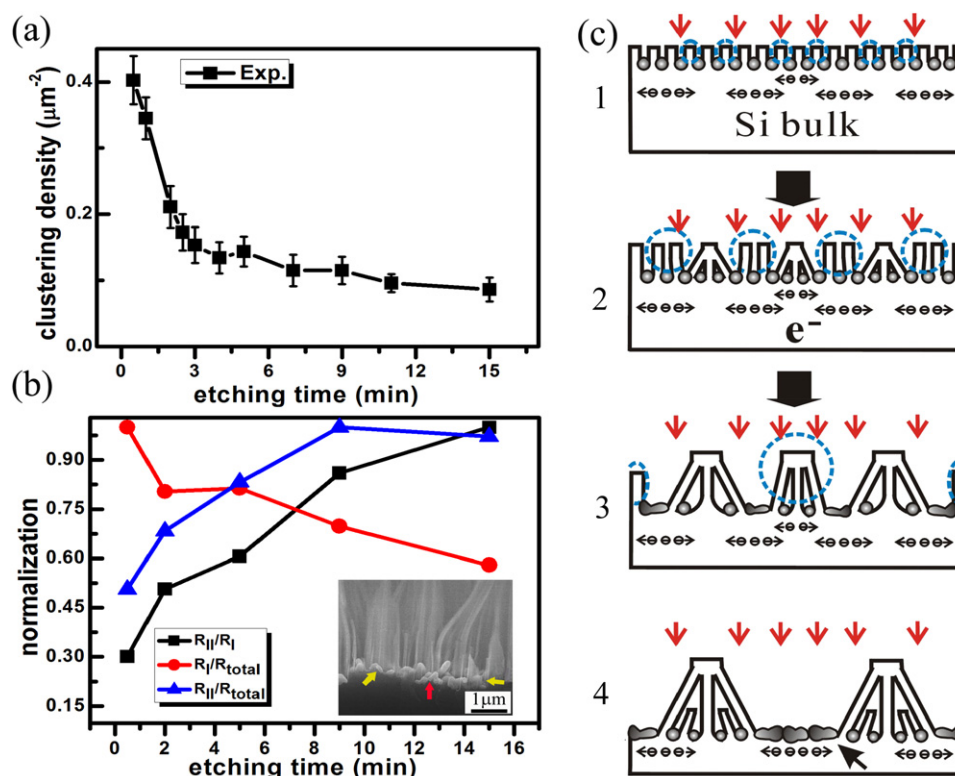


Figure 8. *In situ* analysis and schematic illustration of the SiNW clustering process. (a) Clustering density versus etching time. (b) Ag relative atomic percentage (normalized) evolution with etching time for three regions. R_{total} , R_I and R_{II} stand for the concentrations on average, at the cone center and in the inter-cone area, respectively, as marked in figure 7(h). The inset is an SEM image of SiNWs etched for 15 min with Ag particles. (c) The steps of the morphology change of the SiNWs under illumination: (1) the Ag deposition step before etching; (2) at the very beginning of the reaction, with illumination; the number of electrons is higher where more light is absorbed; (3) lateral movement of the etching front and disappearance of certain clustering SiNWs; (4) lateral movement of the etching front, with mass transport of Ag; the dashed arrow indicates the Ag enrichment.

words, the inclination of the wires in the outer area of the cones was more likely to be induced by the moving trace of the reaction front, i.e., the etching fronts under illumination would no longer move vertically as they do under dark conditions. From the same aspect, the aggregation or ‘clustering of the wires’ on top of the conic structures derives from this diverted etching as well. This can also be seen from the closer top view in figures 7(e) and (f), in which an inclination with a certain curvature appeared as a ‘carving’ effect. More important evidence has come from the measurement of the Ag distribution during the reaction. As a normal assumption, the initial distribution and average coverage of Ag are identical for samples with the same conditions. A certain number of Ag particles stay at the reaction fronts at the bottom of the Si wires. If the above proposed process were true, then due to the motion of the reaction front, a mass transport of Ag should take place, i.e., the motion of Ag will not only be vertical, but also lateral along the surface. Therefore, as the reaction continues, a local enrichment of Ag should be discovered between the two conic clustering structures, where reaction fronts moving in opposite directions collide; meanwhile, due to the same effect, a relative decrease of the amount of Ag should take place in the central area of each cone. In this experiment, we have verified this with EDX measurements and the predicted mass redistribution of Ag

was confirmed. Since the average coverage of Ag decreased as the reaction continued due to chemical dissolution, the local Ag concentration was divided by the average value. For instance, as the experiment was proceeding, the Ag in region I (clustering center) decreased with the reaction and that in region II (inter-clustering area) relatively increased with the reaction (figure 8(b)). For reference, an SEM photo is presented in the inset of figure 8(b), with the yellow and red arrows indicating regions I and II, respectively. The detailed data and calculation can be found in tables S1 and S2 in the supporting information (available at stacks.iop.org/Nano/25/025602/mmedia). However, if we consider the ‘bending’ model, this mass redistribution is not likely to take place. For a similar reason, we can conclude that the reduction of the clustering density in figure 7 is due to the etching effect on some clustered silicon nanowires while others survived and continued to grow. However, the origin of the initial lateral movement of the outer reaction fronts still remains a question. A sound explanation could be related to the influence of photo-generated charge redistribution [38].

Therefore, a more likely picture than the ‘bending’ model can be drawn out in this experiment. Initially, very short SiNWs were formed with the mechanism proposed at the beginning of this section. When light illuminated this surface, electrons were excited from the valence band to the

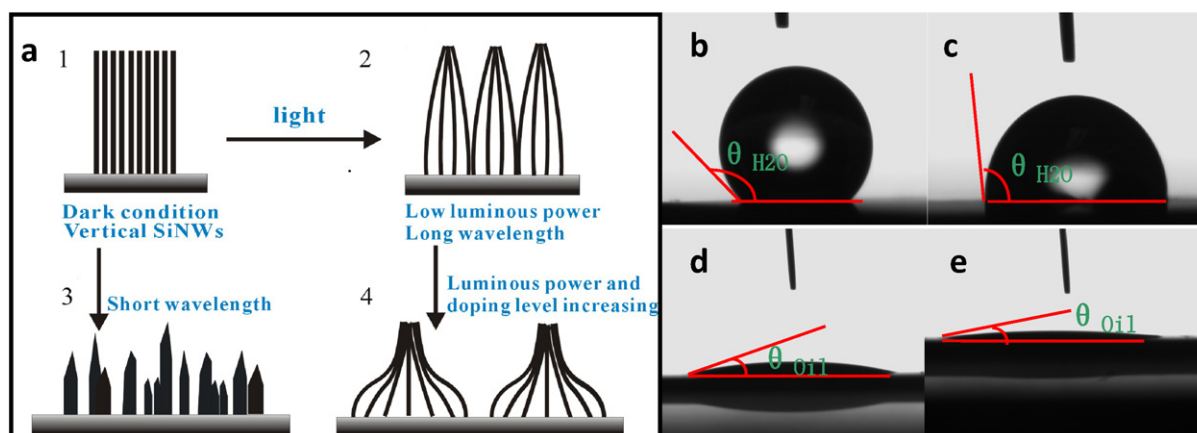


Figure 9. (a) Morphology obtained under different illumination conditions: (1) dark conditions, (2) under low illumination power and long wavelength, (3) under short wavelength, (4) under high illumination power and high doping level. (b)–(e) Hydrophobic and oleophilic characterization of N100 1–10 Ω cm SiNWs with HF treatment. (b), (c) Hydrophobic characterization of SiNWs fabricated (b) without illumination, $\theta_{H_2O} = 137.2^\circ$, (c) with illumination (20 mW, 650 nm), $\theta_{H_2O} = 92.5^\circ$. (d), (e) Oleophilic characterization of SiNWs fabricated (d) without illumination, θ_{oil} (of silicone oil) = 16.4° , (e) with illumination (20 mW, 650 nm), $\theta_{oil} = 11.3^\circ$.

conduction band, and thus the driving force for reduction of Ag^+ became larger [37]. As there would normally be a difference in the incident light in some neighboring inter-column areas, a density gradient of light-induced electron–hole pairs was created. Due to this lateral density gradient at the Si surface, lateral etching could take place at the reaction front (figure 8(c)) [13]. When this process continued, an inclined nanowire was formed. Considering a larger scale, in an area surrounded by several areas with higher electron density, a cone like structure could be formed. In the meantime, Ag was transported into the area with more electrons and became enriched in the area between two cones (indicated by the dashed arrow in step 4). As also depicted in step 4, new SiNW could also develop where the expansions were large enough.

Furthermore, in the area with higher electron densities and more Ag content, the etching rate was relatively enhanced. The enhanced etching process reduced the lengths of local SiNWs and thus reduced their absorption of light energy [1, 39, 40]. Hence, more electrons were created and this process was self-promoted. Therefore, as the cone developed, the column between the cones disappeared, as indicated by the dashed circle in steps 1–3. When the reaction continued, the inclination continued and more cones were destroyed. Therefore, as a general result, we can see the growing size of the clustering and reduced clustering density. Besides, under fixed chemical conditions, this lateral effect is strongly dependent on the photon energy, photon number and doping level of the substrate [22, 41]. The light-induced potential becomes larger if these factors are greater, which accelerates the lateral etching. This can explain the behavior of the deflection angle and the clustering density that we have observed previously. As a general result, we can see that the dimensional parameters of the SiNWs can be effectively modulated by simple factors (figure 9(a)).

Additionally, if the photon energy of the incident light is much higher than the Si bandgap so that it can provide the electrons of the Si with extra energy to have a quick

reaction with the oxidative agent, then the Si can be directly etched by the solution without contact with the silver particles. Therefore the etching process will not only occur at the bottom with the assistance of the Ag but also at the upper part of the nanowires due to the strong etching at the top [31]; the conic clustering cannot be formed and only columns can be left ('bamboo shoot' like pattern). This is also one possible factor that caused the contradictory behavior of the nanowire growth when varying the photon number and energy. If only the number of photons is increased and the energy remains unchanged, then the direct H_2O_2 etching is weak while the prominent parts of the nanowire bunches are easier to etch, which leaves a smoothed or 'melt-down' like surface on top of those clustered nanowires.

5. Potential applications and future work

As discussed above, interesting results have been found from phenomenological and mechanistic studies on the photo-induced morphological and structural change during SiNW formation by light-modulated MACE. Although some questions still remain, the results suggest their certain involvement in current and future research in materials science. Firstly, the morphological change of the nanopillar type array would naturally suggest its relationship with the amphiphilic (hydrophilicity as well as oleophilicity) properties of material surfaces, which are related to applications such as antifogging, self-cleaning and platforms for chemical reactions [42–45]. As a preliminary study, wettability characterization has been carried out in samples (N100 1–10 Ω cm) etched without and with illumination (650 nm, 20 mW). To see the difference more clearly, these samples were dipped into HF solution to remove the oxide layer before the characterization; otherwise the contact angles would all be very close to 0 and be hard to distinguish. As shown by figure 9, the light-modulated SiNWs have significantly smaller contact angles for both water and

silicone oil than the ones without illumination, indicating an enhancement in amphiphilicity and potential amphiphilic applications based on a SiNW substrate.

Moreover, the inclination and clustering in the nanowire arrays have been proved to provide latent enhancement in molecular sensing and light absorption and to possess special mechanical properties [46–50]. For example, SiNWs with orientations other than perpendicular have been reported to be useful for light capture in electro-optic devices or bio-molecule docking in biosensors due to their large sidewall area against normal incidence [47]. Applications can also be found for mechanical sensors [49], or in electro-optic devices due to significant enhancement in the electromagnetic field [46]. Based on the studies of porosity in section 3.5, more detailed research on the porosity of SiNWs might be worthwhile for potential applications as biosensors and light-emitting devices. Finally, the mechanism presented in this experiment under illumination might also offer new comprehension of related processes and a novel structural modification method in MACE. For other noble metals such as Au and Pt, the etching in light-modulated MACE might be stronger and weaker than Ag, respectively, due to the difference in redox potential of these particles ($R_{\text{Au}} > R_{\text{Ag}} > R_{\text{Pt}}$) [8, 33, 51]. Similar mechanisms may also exist in other etching systems [26, 27, 30], and investigation of the mass transport of metals could help to explain and resolve the coalescence of metal nuclei in the Au/Si system and random movement of Pt particles in the Pt/Si system [8, 33, 51].

6. Conclusion

In this paper, we have demonstrated that it is possible to realize morphology control in the formation of SiNWs via modulation of the incident light. Concentric inclination and clustering of SiNWs can be formed with adjustable angle and density, respectively, by varying the illumination power and photon energy. Regarding the origin of those phenomena, detailed mechanistic studies have ruled out the ‘bending model’, in which the morphological change is mainly due to mechanical deformation under the chemical etching effect [25]. Strong evidence from the time evolution experiments on the SiNWs has proved that the main origin of the nanowire inclination and clustering is preferential lateral movement of the reaction fronts at the bottom of the SiNWs. A sound reason for the non-vertical movement of the etching front might be the additional electric field from the inhomogeneous distribution of photo-generated electron–hole pairs at the Si surface in different areas, which is further influenced by the morphological change itself. This study has not only elucidated fundamental aspects of the mechanism of SiNW formation, but also provided prospective applications and new routes for modulation in other noble metal etching systems and similar nanostructure fabrication processes.

Acknowledgments

This work was supported by the National Major Basic Research Project of 2012CB934302, Natural Science Foundation of China under contracts 11204176, 11174202 and 61234005.

References

- [1] Peng K Q and Lee S-T 2011 *Adv. Mater.* **23** 198
- [2] Hochbaum A I, Chen R, Delgado R D, Liang W, Garnett E C, Najarian M, Majumdar A and Yang P 2008 *Nature* **451** 163
- [3] Chan C K, Peng H, Liu G, McIlwrath K, Zhang X F, Huggins R A and Cui Y 2007 *Nature Nanotechnol.* **3** 31
- [4] Qu Y, Liao L, Li Y, Zhang H, Huang Y and Duan X 2009 *Nano Lett.* **9** 4539
- [5] Cui Y, Wei Q, Park H and Lieber C M 2001 *Science* **293** 1289
- [6] Qu Y, Zhong X, Li Y, Liao L, Huang Y and Duan X 2010 *J. Mater. Chem.* **20** 3590
- [7] Wagner R and Ellis W 1964 *Appl. Phys. Lett.* **4** 89
- [8] Huang Z, Geyer N, Werner P, de Boor J and Gösele U 2011 *Adv. Mater.* **23** 285
- [9] Hsu C M, Connor S T, Tang M X and Cui Y 2008 *Appl. Phys. Lett.* **93** 133109
- [10] Lu X, Hanrath T, Johnston K P and Korgel B A 2003 *Nano Lett.* **3** 93
- [11] Li X and Bohn P W 2000 *Appl. Phys. Lett.* **77** 2572
- [12] Peng K, Xu Y, Wu Y, Yan Y, Lee S T and Zhu J 2005 *Small* **1** 1062
- [13] Peng K, Lu A, Zhang R and Lee S T 2008 *Adv. Funct. Mater.* **18** 3026
- [14] Huang Z, Zhang X, Reiche M, Liu L, Lee W, Shimizu T, Senz S and Gösele U 2008 *Nano Lett.* **8** 3046
- [15] Huang Z, Fang H and Zhu J 2007 *Adv. Mater.* **19** 744
- [16] Huang J, Chiam S Y, Tan H H, Wang S and Chim W K 2010 *Chem. Mater.* **22** 4111
- [17] Chern W et al 2010 *Nano Lett.* **10** 1582
- [18] Balasundaram K et al 2012 *Nanotechnology* **23** 305304
- [19] Huang Z, Shimizu T, Senz S, Zhang Z, Zhang X, Lee W, Geyer N and Gösele U 2009 *Nano Lett.* **9** 2519
- [20] Zhang M L, Peng K Q, Fan X, Jie J S, Zhang R Q, Lee S T and Wong N B 2008 *J. Phys. Chem. C* **112** 4444
- [21] Kim J, Han H, Kim Y H, Choi S H, Kim J C and Lee W 2011 *ACS Nano* **5** 3222
- [22] To W K, Tsang C H, Li H H and Huang Z 2011 *Nano Lett.* **11** 5252
- [23] Lai C Q, Thompson C V and Choi W K 2012 *Langmuir* **28** 11048
- [24] Duan H G and Berggren K K 2010 *Nano Lett.* **10** 3710
- [25] Lee D H, Kim Y, Doerk G S, Laboriante I and Maboudian R 2011 *J. Mater. Chem.* **21** 10359
- [26] Kim J K, Kim Y H, Choi S-H and Lee W 2011 *ACS Nano* **5** 5242
- [27] Wang D, Ji R, Du S, Albrecht A and Schaaf P 2013 *Nanoscale Res. Lett.* **8** 42
- [28] Peng K, Fang H, Hu J, Wu Y, Zhu J, Yan Y and Lee S 2006 *Chem.—Eur. J.* **12** 7942
- [29] Geyer N, Fuhrmann B, Huang Z, de Boor J, Leipner H S and Werner P 2012 *J. Phys. Chem. C* **116** 13446
- [30] Kim Y, Tsao A, Lee D H and Maboudian R 2013 *J. Mater. Chem. C* **1** 220
- [31] Osgood R, Sanchez-Rubio A, Ehrlich D and Daneu V 1982 *Appl. Phys. Lett.* **40** 391
- [32] Homay G 1987 *Annu. Rev. Fluid Mech.* **19** 271
- [33] Peng K and Zhu J 2004 *Electrochim. Acta* **49** 2563
- [34] Geyer N et al 2009 *Nano Lett.* **9** 3106
- [35] Xie W Q, Oh J I and Shen W Z 2011 *Nanotechnology* **22** 065704
- [36] Chartier C, Bastide S and Lévy-Clément C 2008 *Electrochim. Acta* **53** 5509
- [37] Norga G, Platero M, Black K, Reddy A, Michel J and Kimerling L 1997 *J. Electrochem. Soc.* **144** 2801
- [38] Niu H, Matsuda T, Sadamatsu H and Takai M 1976 *Japan. J. Appl. Phys.* **15** 601
- [39] Hu L and Chen G 2007 *Nano Lett.* **7** 3249
- [40] Li J, Yu H, Wong S M, Li X, Zhang G, Lo P G-Q and Kwong D-L 2009 *Appl. Phys. Lett.* **95** 243113

- [41] Hochbaum A I, Gargas D, Hwang Y J and Yang P 2009 *Nano Lett.* **9** 3550
- [42] Zhang L W, Dillert R, Bahnemann D and Vormoor M 2012 *Energy Environ. Sci.* **5** 7491
- [43] Wang R, Hashimoto K, Fujishima A, Chikuni M, Kojima E, Kitamura A, Shimohigoshi M and Watanabe T 1997 *Nature* **388** 431
- [44] Watanabe T, Nakajima A, Wang R, Minabe M, Koizumi S, Fujishima A and Hashimoto K 1999 *Thin Solid Films* **351** 260
- [45] Baek S and Na K 2013 *Colloids Surf. B* **101** 493
- [46] Zhang B, Wang H, Lu L, Ai K, Zhang G and Cheng X 2008 *Adv. Funct. Mater.* **18** 2348
- [47] Aschenbrenner T *et al* 2011 *Phys. Status Solidi b* **248** 1787
- [48] Yun S H, Wu J Z, Dibos A, Zou X D and Karlsson U O 2006 *Nano Lett.* **6** 385
- [49] Min Y, Akbulut M, Belman N, Golan Y, Zasadzinski J and Israelachvili J 2007 *Nano Lett.* **8** 246
- [50] Azeredo B P *et al* 2013 *Nanotechnology* **24** 225305
- [51] Peng K Q and Zhu J 2003 *J. Electroanal. Chem.* **558** 35